Letter

Anderson localization transition in a robust $\mathcal{PT}$-symmetric phase of a generalized Aubry-André model

Sebastian Schiffer,* Xia-Ji Liu, Hui Hu, and Jia Wang†
Centre for Quantum Technology Theory, Swinburne University of Technology, Melbourne 3122, Australia

(Received 20 October 2020; accepted 15 January 2021; published 29 January 2021)

We study a generalized Aubry-André model that obeys $\mathcal{PT}$ symmetry. We observe a robust $\mathcal{PT}$-symmetric phase with respect to system size and disorder strength, where all eigenvalues are real despite the Hamiltonian being non-Hermitian. This robust $\mathcal{PT}$-symmetric phase can support an Anderson localization transition, giving a rich phase diagram as a result of the interplay between disorder and $\mathcal{PT}$ symmetry. Our model provides a perfect platform to study disorder-driven localization phenomena in a $\mathcal{PT}$-symmetric system.

DOI: 10.1103/PhysRevA.103.L011302

I. INTRODUCTION

Out-of-equilibrium open quantum systems are ubiquitous, where energy, particles, and information can transfer to or from the surrounding environment. In some limits, non-Hermitian Hamiltonians can well describe the quantum behavior of these systems [1–10]. The presence of complex eigenvalues of non-Hermitian Hamiltonians is a direct consequence of the nonpreservation of probability due to loss and gain. However, non-Hermitian Hamiltonians that exhibit parity-time ($\mathcal{PT}$) symmetry can still possess a purely real spectrum, indicating that the loss and gain are coherently balanced [11]. $\mathcal{PT}$ symmetry refers to the invariance of the Hamiltonian under a combined parity ($\mathcal{P}$) and time-reversal ($\mathcal{T}$) transformation, but not necessarily with $\mathcal{P}$ and $\mathcal{T}$ separately. Furthermore, a spontaneous $\mathcal{PT}$-symmetry breaking may occur when the degree of non-Hermiticity is large enough, where eigenvalues that come in complex-conjugate pairs appear. We usually name the real (complex) spectral phase as a $\mathcal{PT}$-symmetric (-broken) phase.

$\mathcal{PT}$ symmetry has become an active research area since the original work by Bender and Boettcher [11]. Applications of $\mathcal{PT}$ symmetry have been found in various physics areas, ranging from quantum field theories and mathematical physics [12–15] to solid-state physics [16,17] and optics [18–23]. It has recently attracted intense interest due to the rapid progress in atomic, molecular, and optical (AMO) experiments, where engineered loss and gain is accessible in a controllable manner [23–32]. In particular, the real-to-complex spectral transition ($\mathcal{PT}$ transition) has been observed both in classical [33] and quantal [34] systems.

Another theoretical concept that has gained a lot of attention recently, thanks to experimental developments in photonic crystals [35–39] and ultracold atoms [40,41], is Anderson localization [42]. Anderson localization refers to the absence of a particle's diffusion induced by disorder. In a one-dimensional (1D) lattice model, an on-site cosine modulation incommensurate with the underlying lattice can be regarded as a highly correlated disorder, in a loose qualitative sense, and hence is sometimes called quasidisorder. Aubry and André (AA) showed that a 1D tight-binding model with a quasidisorder has a self-dual symmetry and manifests as a localization phase transition for all eigenstates at a critical modulation strength [43]. This seminal work stimulated extensive theoretical and experimental investigations in various generalized AA models [44–56].

A localization transition can also occur in a non-Hermitian Hamiltonian system, such as non-Hermitian extensions of the AA model [57–59] and the Hatano-Nelson model with asymmetric hopping amplitudes [60–63]. A very recent study gives an interesting topological interpretation for the existence of the localization transition in the Hatano-Nelson model [64]. However, whether an Anderson localization transition can exist in a $\mathcal{PT}$-symmetric Hamiltonian remains elusive. On the one hand, an exponential localization state induced by disorder requires a very large system size and can only be stable in the $\mathcal{PT}$-symmetric phase. On the other hand, an uncorrelated disorder usually does not respect $\mathcal{PT}$ symmetry, making the $\mathcal{PT}$-symmetric phase disappear for an arbitrarily weak disorder strength [65,66]. Even in a few studies that use an engineered $\mathcal{PT}$-symmetric disorder, the $\mathcal{PT}$-symmetric phase is still generally very fragile in the sense that it exists only for an exponentially small non-Hermiticity parameter in the large system size limit [16,67–69]. Interestingly, the $\mathcal{PT}$-symmetric phase becomes robust if an asymmetric hopping is introduced, implying that Anderson localization might exist [67,70–72].

II. GENERALIZED AA MODEL

We study a generalized AA model with commensurate modulation in both on-site potentials and asymmetric imaginary hopping terms in this work. The Hamiltonian of the one-dimensional (1D) generalized AA model that we consider

*sschiffer@swin.edu.au
†jiawang@swin.edu.au

here is given by

$$\hat{H} = \sum_{j=1}^{N} [t_j \hat{c}_{j+1}^{\dagger} \hat{c}_j + t_{j+1} \hat{c}_j^{\dagger} \hat{c}_{j+1} + V_j \hat{c}_j^{\dagger} \hat{c}_j], \tag{1}$$

where $\hat{c}_j^{\dagger}$ (c_j) is the creation (annihilation) operator at site j, and the subindex j should be understood as j (mod N). The on-site modulation is given by $V_j = 2V_0 \cos(2\pi\beta j + \varphi)$, and the hopping is complex and asymmetric: $t_j = t + i\gamma_0 \sin(2\pi\beta j + \varphi) \neq t_{j+1}^{*}$. Here, V_0 is the quasidisorder strength and γ_0 controls the non-Hermiticity. We also choose $\beta = M/N$, where M and N are two adjacent Fibonacci numbers, which are mutually prime. When $\gamma_0 = 0$, the model Hamiltonian reduces back to the traditional AA model with hopping amplitude t.

We analytically prove that this Hamiltonian is $\mathcal{PT}$ symmetric for a set of modulation phase factors $\varphi = \varphi_{\mathcal{PT}} \equiv m\pi/N$, where m are odd (integer) numbers if N is even (odd) [73]. Surprisingly, we numerically observe that under some conditions, the system's spectrum remains (up to the numerical accuracy) all real or complex-conjugate paired for *any arbitrary* φ. We test the violation of $\mathcal{PT}$ symmetry of our Hamiltonian by defining a measure that vanishes if all eigenenergies E_k are either real or complex-conjugate paired,

$$S_{\mathcal{PT}} = \frac{1}{N}\sum_{k}^{N} |\mathrm{Im}(E_k)| \prod_{m\neq k}^{N} [1 - \delta(E_k, E_m)] + \frac{1}{2N}\sum_{k}^{N}\sum_{m\neq k}^{N} \delta(E_k, E_m)|\mathrm{Im}(E_k) + \mathrm{Im}(E_m)|, \tag{2}$$

where $\delta(E_k, E_m) = 1$ if the difference of the real parts is small enough, i.e., $|\mathrm{Re}(E_k) - \mathrm{Re}(E_m)| < \epsilon_{\mathrm{tol}}$, and 0 otherwise. We choose a tolerance $\epsilon_{\mathrm{tol}} = 10^{-4} V_0$ for the numerical implementation. Here, we use Re (Im) to denote the real (imaginary) part. Figure 1(a) shows the behavior of the maximum of $S_{\mathcal{PT}}/V_0$ over φ as a function of N for some typical parameters to characterize whether the spectrum is purely real. Our numerical result shows that $S_{\mathcal{PT}}/V_0$ are always vanishingly small for even chains (i.e., N is even). For long enough ($N > 55$) odd chains, $S_{\mathcal{PT}}/V_0$ is also as small as the numerical precision except at the ray $\{t = 0, \gamma_0 > V_0\}$ in the t–γ_0 parameter space, which is called "special ray" for convenience hereafter. We remark here that for analyzing the disorder-driven localization transition, it is vital that the spectrum remains purely real or complex-conjugate paired for arbitrary φ since it allows us to average over the phase factor φ to emulate disorder realization. Hereafter, unless specified otherwise, we always average observables over φ and denote the average as $\langle\cdot\rangle$, except at the special ray, where we only calculate for $\varphi = \varphi_{\mathcal{PT}}$.

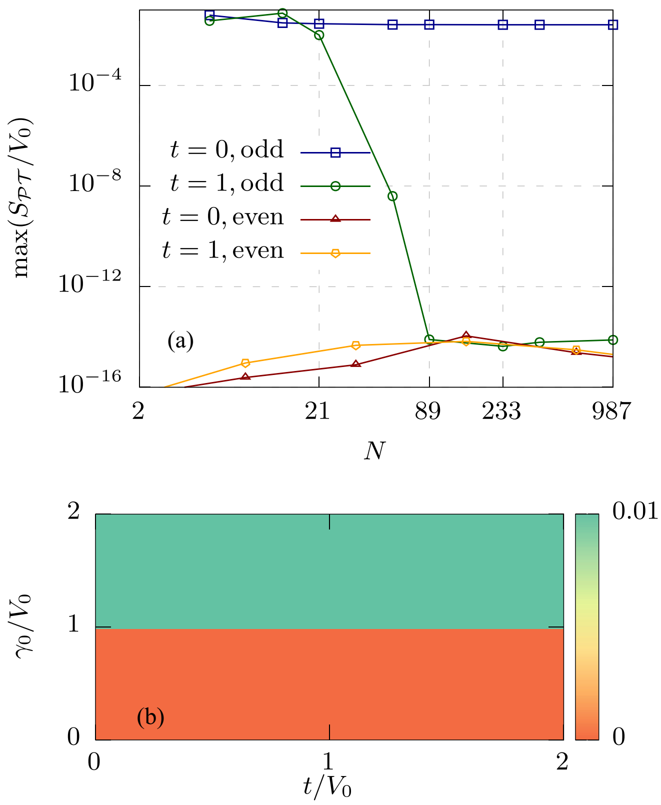

FIG. 1. (a) Maximum violation of the $\mathcal{PT}$ symmetry $\max(S_{\mathcal{PT}}/V_0)$ for even and odd chains at $\gamma_0 = 2$, $t = 0$, and $t = 1$. (b) $\langle I_{\mathcal{PT}}\rangle/V_0$ reveals the robust $\mathcal{PT}$-symmetric phase existing for $\gamma_0 < 1$ for arbitrary t/V_0.

III. $\mathcal{PT}$-BROKEN PHASE

For $\mathcal{PT}$-symmetric systems, the $\mathcal{PT}$ symmetry might be spontaneously broken if the degree of non-Hermiticity is large enough [11]. In our system, we explore the parameter space to find both symmetry-broken and -unbroken regions. As the appearance of complex-conjugate pairs in the spectrum of a $\mathcal{PT}$-symmetric system indicates the broken phase, we define a $\mathcal{PT}$-symmetry indicator as the sum over the absolute values of the imaginary parts of the spectrum,

$$I_{\mathcal{PT}} = \sum_{k} |\mathrm{Im}(E_k)|, \tag{3}$$

which vanishes if the spectrum is purely real. We observe that $\langle I_{\mathcal{PT}}\rangle/V_0$ abruptly changes from finite to vanishingly small at the vicinity of $\gamma_0 = V_0$, irrespective of the value of t/V_0, marking the boundary between the $\mathcal{PT}$-symmetric and -broken phases, as depicted in Fig. 1(b). The fact that a $\mathcal{PT}$ transition occurs at $\gamma_0 = V_0$ for arbitrary t/V_0 implies that the $\mathcal{PT}$-symmetric phase in our system is robust against strong disorder. We have also confirmed that this $\mathcal{PT}$-phase diagram is essentially unchanged for larger N, indicating the robustness against system size. The robustness of the $\mathcal{PT}$-symmetric phase in our system is in stark contrast to most of the previous studies, where the $\mathcal{PT}$-symmetric phase becomes exponentially fragile in the presence of disorder.

IV. LOCALIZATION

Next, we investigate the system for its localization behavior. A widely used measure for localization is the inverse participation ratio (IPR) [74]. For a normalized wave function $\psi(j)$ of a Hermitian Hamiltonian, the IPR is defined as the summation of the probability over all the sites, $\sum_j p(j)^2 \equiv \sum_j |\psi(j)|^4$. In the case of non-Hermitian Hamiltonians, the

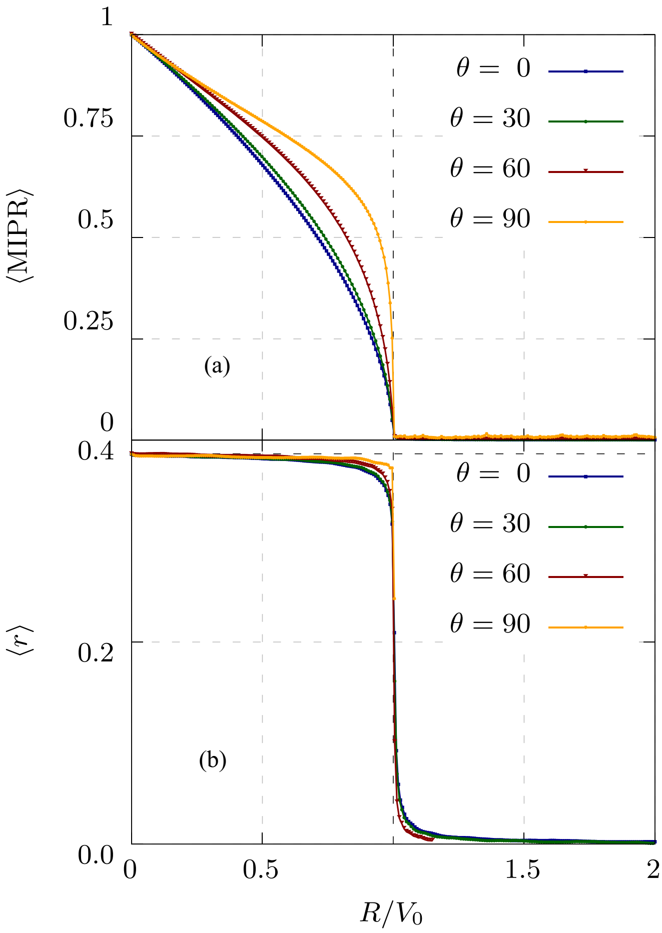

FIG. 2. ⟨MIPR⟩ and ⟨r⟩ as a function of $R = \sqrt{t^2+\gamma_0^2}$. (a) The ⟨MIPR⟩ at several different $\theta = \tan^{-1}(\gamma_0/t)$, indicating that the localization transition occurs at $R = V_0$ for all θ. (b) The gap statistics $\langle r\rangle \approx 0.38$, the Poisson distribution value, in the strong disorder limit $t/V_0 \to 0$, and a rapid decay at the localization transition boundary.

left and right eigenvectors can be orthonormalized in the sense that $\sum_j \psi_m^L(j)^*\psi_k^R(j) = \delta_{mk}$, where $p_k^{LR}(j) = \psi_k^L(j)^*\psi_k^R(j)$ plays a similar role as the probability at site j. Thus we define the IPR measure as [75]

$$\mathrm{IPR}_{LR}\,(E_k) = \left\{\frac{\left[\sum_j \left|\psi_k^L(j)\psi_k^R(j)\right|\right]^2}{\sum_j \left|\psi_k^L(j)\psi_k^R(j)\right|^2}\right\}^{-1}, \tag{4}$$

which varies from being $O(1/N)$ for eigenfunctions smeared uniformly over all sites to $O(1)$ for those localized near a specific site. Therefore, the IPR can serve as an indicator for the localization transition. Averaging the IPR over all eigenfunctions and all quasidisorder realizations gives the mean inverse participation ratio, $\langle\mathrm{MIPR}\rangle = \langle\sum_k \mathrm{IPR}_{LR}(E_k)/N\rangle$ [73]. Figure 2(a) shows the ⟨MIPR⟩ as a function of $R = \sqrt{t^2+V_0^2}$ for various $\theta = \mathrm{atan}(\gamma_0/t) \in [0^\circ, 90^\circ]$. These calculations are carried out for $N = 1597$, where the numeric is well converged. The ⟨MIPR⟩ monotonically decreases from one to zero in the regime $R/V_0 \in [0, 1]$ and slower for larger θ. The ⟨MIPR⟩ also essentially remains zero in the regime $R > V_0$ for any θ. In the t–γ_0 parameter space, R/V_0 can be recognized as the distance to the origin, and θ as the angle to the t axis. Therefore, the localization boundary is located at the quarter-circle arc $\sqrt{t^2+\gamma_0^2} = V_0$, which is also illustrated in the phase diagram in Fig. 3(a).

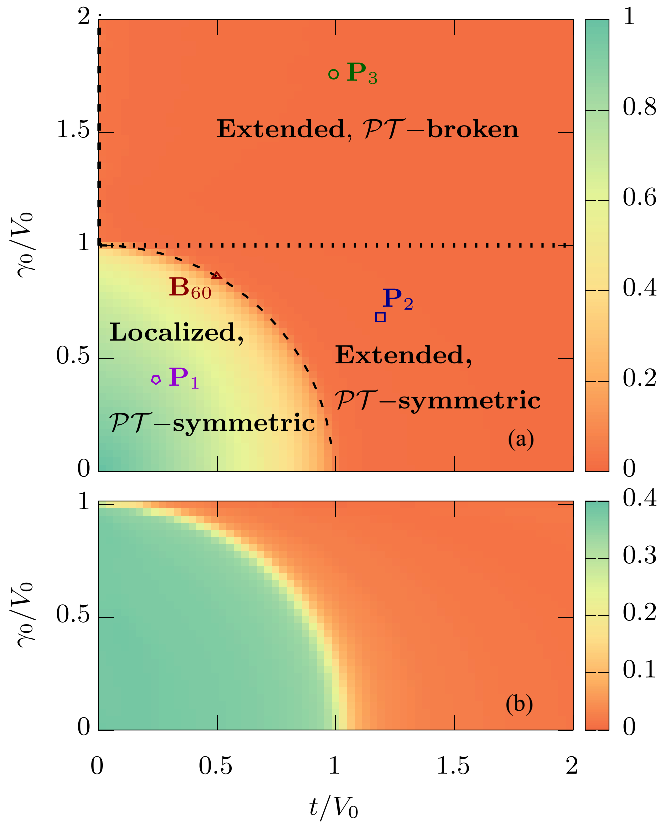

FIG. 3. Phase diagrams of the system for $N = 233$. (a) The ⟨MIPR⟩ and (b) gap statistics ⟨r⟩, both of which identify a localized phase within the quarter circle $\sqrt{t^2+\gamma_0^2} \leqslant V_0$. The localization-transition and $\mathcal{PT}$-transition boundaries are also indicated in (a) by the thin dashed curve and the dotted line, respectively. A thick dashed line illustrates the "special ray" $\{t = 0, \gamma > 1\}$ detailed in the main text. We also mark several specific points P_1, P_2, P_3, and B_{60} in different phase regimes, which correspond to $\{t/V_0, \gamma_0/V_0\} \approx \{0.24, 0.42\}$, $\{1.2, 0.69\}$, $\{1.0, 1.74\}$, and $\{\cos(60^\circ), \sin(60^\circ)\}$. We exemplify properties of different phases on these points as detailed in the main text.

We also perform an energy gap statistic analysis to diagnose the localization transition. As the energies can be complex in the $\mathcal{PT}$-broken regime, we restrict this analysis to the region $\gamma_0 \leqslant V_0$, where the averaged level spacing ratio is well defined: $r = \sum_k r_k/(N-1)$ and

$$r_k = \frac{\min(\delta_{k+1}, \delta_k)}{\max(\delta_{k+1}, \delta_k)}, \quad \delta_k = E_{k+1} - E_k. \tag{5}$$

In the deeply localized region $R/V_0 \to 0$, $\langle r\rangle \to \langle r\rangle_{\mathrm{Poisson}} = 2\ln(2) - 1 \approx 0.3863$ for a Poisson distribution [76,77], as shown in Fig. 2(b). In the deep extended region $R/V_0 \to \infty$, an asymptotic degeneracy emerges due to the periodic boundary condition and vanishing disorder. Consequently, $\langle r\rangle \to 0$ in this limit, instead of $\langle r\rangle_{\mathrm{GOE}} \approx 0.5307$ for a Gaussian orthogonal ensemble as one might naïvely assume. As ⟨r⟩ also changes rapidly at $R = V_0$, this assures one of a localization-transition boundary, as shown in Fig. 3(b).

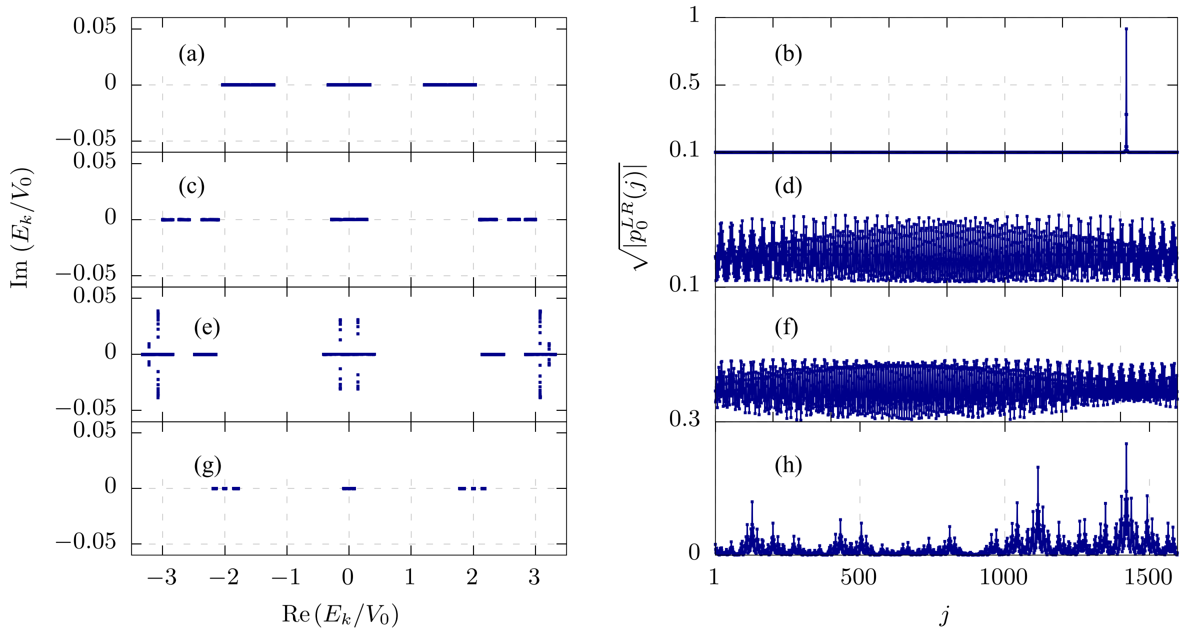

FIG. 4. Energy spectra $\mathrm{Im}(E_k)$ as a function of $\mathrm{Re}(E_k)$ and $\sqrt{|p_0^{LR}(j)|}$ of the state with $E_0 \approx 0$ for $N = 1597$ for the different sets of parameters marked in Fig. 3(a). The spectra are shown in (a), (c), (e), and (g) and the wave functions are shown in (b), (d), (f), and (h) for P_1, P_2, P_3, and B_{60}, respectively.

Our main results are summarized and illustrated in the phase diagrams in Fig. 3: (1) a robust $\mathcal{PT}$-symmetric phase exists for large system sizes and arbitrary disorder strength; (2) a disorder-driven localization transition occurs within the $\mathcal{PT}$-symmetric phase on a quarter-circle arc $\sqrt{t^2 + \gamma_0^2} = V_0$ as the phase boundary; (3) along this phase boundary and $t = 0$, $\gamma_0 \geqslant V_0$, the system shows critical behavior; and (4) in the $\mathcal{PT}$-broken phase, the eigenwave functions are extended.

V. MULTIFRACTAL ANALYSIS

Next, we investigate the spectra and wave functions at different phase regimes. As some typical examples, we show E_k and $\sqrt{|p_0^{LR}(j)|}$ in Fig. 4 for four sets of $\{t, \gamma_0\}$ marked in Fig. 3(a): P_1 in the localized phase, P_2 in the $\mathcal{PT}$-symmetric and extended phase, P_3 in the $\mathcal{PT}$-broken and extended phase, and B_{60} at the localization-transition boundary. Here, $\sqrt{|p_0^{LR}(j)|}$ corresponds to the eigenstate with eigenenergy E_0 closest to 0, which is near the center of the spectrum. The numerical examples are calculated using $\varphi \approx 0.157$ and $N = 1597$. Figures 4(a) and 4(b) shows a purely real spectrum and localized wave function at P_1. At P_2, the spectrum is also purely real, as shown in Fig. 4(c), but the wave function spreads across all sites in Fig. 4(d). Complex-conjugate pairs show up in the spectrum in Fig. 4(e), and the extended wave function is shown in Fig. 4(f) for P_3. In Figs. 4(g) and 4(h), the spectrum and wave function for $R = V_0$ and $\theta = 60^\circ$ (B_{60}) are depicted. As this point is at the phase boundary between the localized and extended region, we expect the system to show critical behavior. Indeed, looking at the wave function, we can see that it is not completely smeared over the chain. The peaks are larger and the wave function looks less dense as for the extended states in Figs. 4(d) and 4(f). This is a signature of a multifractal wave function. To investigate the critical behavior of the system further, we employ a multifractal analysis.

To analyze the scaling behavior of the wave functions, we apply the approach detailed by Refs. [49,73,78] and only mention the key steps here. For a lattice with length $N = F_n$, where F_n is the nth Fibonacci number, a scaling index α_j can be defined as

$$\left|p_0^{LR}(j)\right| = F_n^{-\alpha_j}. \tag{6}$$

For an extended wave function, $\alpha_j \sim 1$ since $|p_0^{LR}(j)| \sim 1/F_n$. For a localized state, on the other hand, $|p_0^{LR}(j)|$ is nonzero only on a finite number of lattice sites. Therefore, $\alpha_j \sim 0$ on these few localized sites and $\alpha_j \to \infty$ on the other sites. For critical wave functions, the index α_j would distribute on a finite interval $[\alpha_{\min}, \alpha_{\max}]$. Hence, we may use $\alpha_{\min}$ in the thermodynamic limit $n \to \infty$ to characterize the scaling behavior: $\alpha_{\min} = 1$ for extended states, $\alpha_{\min} = 0$ for localized states, and $0 < \alpha_{\min} < 1$ for critical states. In the numerical calculations, we average $\alpha_{\min}$ over different quasidisorder configurations for finite n. We fit the data points with a linear function to extrapolate the limit $1/n \to 0$.

We present the results of the multifractal scaling in Fig. 5. In Fig. 5(a), the purple pentagons correspond to P_1 in the localized phase, where the extrapolation reveals $\langle\alpha_{\min}\rangle \to 0$. Both the blue squares and green circles that correspond to P_2 and P_3, respectively, show the trend $\langle\alpha_{\min}\rangle \to 1$, confirming that the wave functions are extended in both phases. At the localization-transition boundary B_{60}, the extrapolation of red triangles gives $\langle\alpha_{\min}\rangle \approx 0.361$ as a signature of the multifractal nature of the critical wave function. In Fig. 5(b), we display the extrapolated value of $\langle\alpha_{\min}\rangle$ as a function of R. $\langle\alpha_{\min}\rangle$ stays at zero for the localized phase region $R < V_0$. At the boundary, the value rises quickly in the critical region until the value assumes the extended one. At the critical point

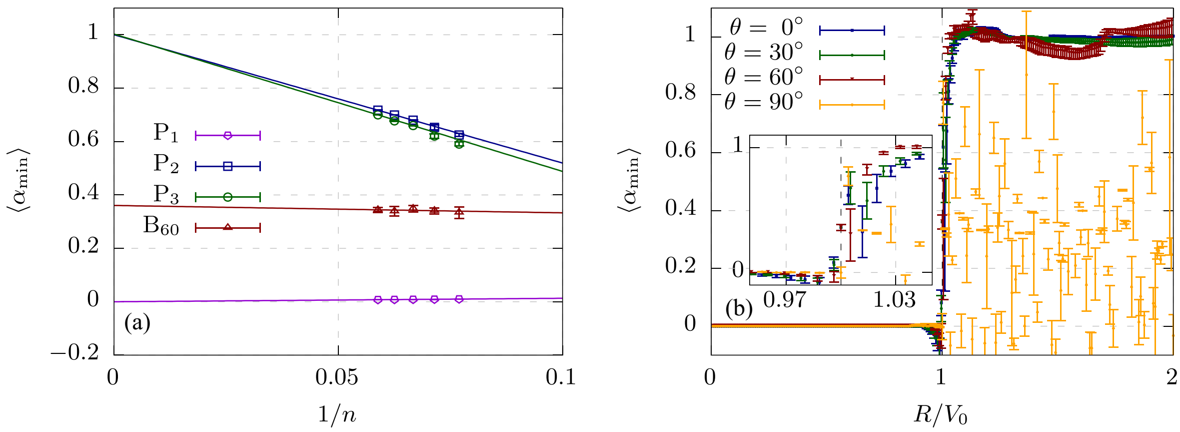

FIG. 5. (a) $\langle\alpha_{\min}\rangle$ for different chain length $N = F_n$ with $n = 13$–17 for P$_1$, P$_2$, P$_3$, and B$_{60}$ defined in Fig. 3(a). Extrapolation of $\langle\alpha_{\min}\rangle$ to the $1/n \to 0$ limit can distinguish extended, localized, and critical phases. (b) The values of $\langle\alpha_{\min}\rangle$ for $1/n \to 0$ obtained from extrapolation for different θ, illustrating the localization transition at $R = V_0$. The inset illustrates a zoom-in near $R = V_0$, emphasizing that the critical indexes $\langle\alpha_{\min}\rangle$ all collapse approximately on 0.36 for different θ, except $\theta = 90°$.

$R = V_0$, the value of $\langle\alpha_{\min}\rangle \approx 0.361 \pm 0.024$ stays constant for all simulated values of θ, except $\theta = 90°$. The good agreement of $\langle\alpha_{\min}\rangle$ between different θ at the critical point can be observed in the inset of Fig. 5(b), where we show the zoomed region around $R = V_0$, revealing the critical region within $R \in [0.96, 1.04]$. We notice that $\theta = 90°$, $R > V_0$ correspond to the "special ray" mentioned earlier, where we do not average over φ, and hence the finite-size effects become more severe. Nevertheless, despite the discontinuity and large error bars of $\alpha_{\min}$ on the "special ray," the wave function can be classified as multifractal since $0 < \alpha < 1$. This implies that the system is critical at $t = 0$ in the $\mathcal{PT}$-broken phase, which will be explored in a more systematic way in future studies.

VI. EXPERIMENTAL REALIZATION

Experimental realization of the $\mathcal{PT}$-symmetric Hamiltonian has been recently achieved in dissipative ultracold-atom systems via investigation of the dynamics conditioned on measurement outcomes [34,79]. Our model Hamiltonian given by Eq. (1) can, in principle, be realized based on ultracold atoms in optical lattices with technologies in currently existing proposals such as engineered dissipation and laser-assisted hopping (see the Supplemental Material for details [73]).

VII. CONCLUSION

We have studied a generalized $\mathcal{PT}$-symmetric AA model. We have observed a $\mathcal{PT}$-symmetric phase $\gamma_0 < V_0$ that is robust against disorder and system size. Furthermore, we have calculated the $\langle$MIPR$\rangle$ and carried out the energy gap statistics to characterize the localized and extended phases. We report a localized phase within a quarter circle, $\sqrt{\gamma_0^2 + t^2} \leqslant V_0$. Additionally, the system features a critical behavior at the localization-transition boundary $R = V_0$ and a special ray $\{R > V_0, \theta = 90°\}$, where we have analyzed fractal behaviors of the wave function.

ACKNOWLEDGMENT

We are grateful to Brendan C. Mulkerin for fruitful discussions. This research was supported by the Australian Research Council's (ARC) Discovery Program, Grant No. DP180102018 (X.-J.L.), Grant No. DP170104008 (H.H.), and Grants No. DE180100592 and No. DP190100815 (J.W.).

[1] V. V. Sokolov and V. G. Zelevinsky, On a statistical theory of overlapping resonances, Phys. Lett. B **202**, 10 (1988).
[2] V. V. Sokolov and V. G. Zelevinsky, Dynamics and statistics of unstable quantum states, Nucl. Phys. A **504**, 562 (1989).
[3] I. Rotter, A continuum shell model for the open quantum mechanical nuclear system, Rep. Prog. Phys. **54**, 635 (1991).
[4] V. V. Sokolov and V. G. Zelevinsky, On a statistical theory of overlapping resonances, Ann. Phys. (NY) **216**, 323 (1992).
[5] H. Carmichael, *An Open System Approach to Quantum Optics* (Springer-Verlag, Heidelberg, 1993).
[6] F. M. Dittes, The decay of quantum systems with a small number of open channels, Phys. Rep. **339**, 215 (2000).
[7] A. J. Daley, Quantum trajectories and open many-body quantum systems, Adv. Phys. **63**, 77 (2014).
[8] Y. Ashida, S. Furukawa, and M. Ueda, Quantum critical behavior influenced by measurement backaction in ultracold gases, Phys. Rev. A **94**, 053615 (2016).
[9] Y. Ashida, S. Furukawa, and M. Ueda, Parity-time-symmetric quantum critical phenomena, Nat. Commun. **8**, 15791 (2017).
[10] L. Jin and Z. Song, Bulk-boundary correspondence in a non-hermitian system in one dimension with chiral inversion symmetry, Phys. Rev. B **99**, 081103(R) (2019).
[11] C. M. Bender and S. Boettcher, Real Spectra in Non-Hermitian Hamiltonians Having $\mathcal{PT}$ symmetry, Phys. Rev. Lett. **80**, 5243 (1998).

[12] C. M. Bender, S. Boettcher, and P. N. Meisinger, PT-symmetric quantum mechanics, J. Math. Phys. (NY) **40**, 2201 (1999).
[13] C. M. Bender, D. C. Brody, and H. F. Jones, Complex Extension of Quantum Mechanics, Phys. Rev. Lett. **89**, 270401 (2002).
[14] C. M. Bender, S. Boettcher, and P. N. Meisinger, Making sense of non-Hermitian Hamiltonians, Rep. Prog. Phys. **70**, 947 (2007).
[15] C. M. Bender, D. C. Brody, and M. P. Müller, Hamiltonian for the Zeros of the Riemann Zeta Function, Phys. Rev. Lett. **118**, 130201 (2017).
[16] O. Bendix, R. Fleischmann, T. Kottos, and B. Shapiro, Exponentially Fragile $\mathcal{PT}$ Symmetry in Lattices with Localized Eigenmodes, Phys. Rev. Lett. **103**, 030402 (2009).
[17] L. Jin and Z. Song, Solutions of $\mathcal{PT}$-symmetric tightbinding chain and its equivalent hermitian counterpart, Phys. Rev. A **80**, 052107 (2009).
[18] R. El-Ganainy, K. G. Makris, D. N. Christodoulides, and Z. H. Musslimani, Theory of coupled optical PT-symmetric structures, Opt. Lett. **32**, 2632 (2007).
[19] K. G. Makris, R. El-Ganainy, D. N. Christodoulides, and Z. H. Musslimani, Beam Dynamics in $\mathcal{PT}$ Symmetric Optical Lattices, Phys. Rev. Lett. **100**, 103904 (2008).
[20] Z. H. Musslimani, K. G. Makris, R. El-Ganainy, and D. N. Christodoulides, Optical Solitons in $\mathcal{PT}$ Periodic Potentials, Phys. Rev. Lett. **100**, 030402 (2008).
[21] S. Longhi, Bloch Oscillations in Complex Crystals with $\mathcal{PT}$ Symmetry, Phys. Rev. Lett. **103**, 123601 (2009).
[22] S. Longhi, Dynamic localization and transport in complex crystals, Phys. Rev. B **80**, 235102 (2009).
[23] A. Guo, G. J. Salamo, D. Duchesne, R. Morandotti, M. Volatier-Ravat, V. Aimez, G. A. Siviloglou, and D. N. Christodoulides, Observation of $\mathcal{PT}$-Symmetry Breaking in Complex Optical Potentials, Phys. Rev. Lett. **103**, 093902 (2009).
[24] C. E. Rüter, K. G. Makris, R. El-Ganainy, D. N. Christodoulides, M. Segev, and D. Kip, Observation of parity-time symmetry in optics, Nat. Phys. **6**, 192 (2010).
[25] A. Regensburger, C. Bersch, M.-A. Miri, G. Onishchukov, D. N. Christodoulides, and U. Peschel, Parity-time synthetic photonic lattices, Nature (London) **488**, 167 (2012).
[26] B. Peng, Ş. K. Özdemir, F. Lei, F. Monifi, M. Gianfreda, G. L. Long, S. Fan, F. Nori, C. M. Bender, and L. Yang, Parity-time-symmetric whispering-gallery microcavities, Nat. phys. **10**, 394 (2014).
[27] L. Feng, Z. J. Wong, R.-M. Ma, Y. Wang, and X. Zhang, Single-mode laser by parity-time symmetry breaking, Science **346**, 972 (2014).
[28] H. Hodaei, M.-A. Miri, M. Heinrich, D. N. Christodoulides, and M. Khajavikhan, Parity-time- symmetric microring lasers, Science **346**, 975 (2014).
[29] B. Zhen, C. W. Hsu, Y. Igarashi, L. Lu, I. Kaminer, A. Pick, S.-L. Chua, J. D. Joannopoulos, and M. Soljačić, Spawning rings of exceptional points out of dirac cones, Nature (London) **525**, 354 (2015).
[30] J. M. Zeuner, M. C. Rechtsman, Y. Plotnik, Y. Lumer, S. Nolte, M. S. Rudner, M. Segev, and A. Szameit, Observation of a Topological Transition in the Bulk of a Non-Hermitian System, Phys. Rev. Lett. **115**, 040402 (2015).
[31] C. Poli, M. Bellec, U. Kuhl, F. Mortessagne, and H. Schomerus, Selective enhancement of topologically induced interface states in a dielectric resonator chain, Nat. Commun. **6**, 6710 (2015).
[32] J. Doppler, A. A. Mailybaev, J. Böhm, U. Kuhl, A. Girschik, F. Libisch, T. J. Milburn, P. Rabl, N. Moiseyev, and S. Rotter, Dynamically encircling an exceptional point for asymmetric mode switching, Nature (London) **537**, 76 (2016).
[33] C. M. Bender, B. K. Berntson, D. Parker, and E. Samuel, Observation of $\mathcal{PT}$ phase transition in a simple mechanical system, Am. J. Phys. **81**, 173 (2013).
[34] J. Li, A. K. Harter, J. Liu, L. de Melo, Y. N. Joglekar, and L. Luo, Observation of parity-time symmetry breaking transitions in a dissipative floquet system of ultracold atoms, Nat. Commun. **10**, 855 (2019).
[35] L. Dal Negro, C. J. Oton, Z. Gaburro, L. Pavesi, P. Johnson, A. Lagendijk, R. Righini, M. Colocci, and D. S. Wiersma, Light Transport Through the Band-Edge States of Fibonacci Quasicrystals, Phys. Rev. Lett. **90**, 055501 (2003).
[36] Y. Lahini, R. Pugatch, F. Pozzi, M. Sorel, R. Morandotti, N. Davidson, and Y. Silberberg, Observation of a Localization Transition in Quasiperiodic Photonic Lattices, Phys. Rev. Lett. **103**, 013901 (2009).
[37] Y. E. Kraus, Y. Lahini, Z. Ringel, M. Verbin, and O. Zilberberg, Topological States and Adiabatic Pumping in Quasicrystals, Phys. Rev. Lett. **109**, 106402 (2012).
[38] M. Verbin, O. Zilberberg, Y. E. Kraus, Y. Lahini, and Y. Silberberg, Observation of Topological Phase Transitions in Photonic Quasicrystals, Phys. Rev. Lett. **110**, 076403 (2013).
[39] M. Verbin, O. Zilberberg, Y. Lahini, Y. E. Kraus, and Y. Silberberg, Topological pumping over a photonic fibonacci quasicrystal, Phys. Rev. B **91**, 064201 (2015).
[40] G. Roati, C. D'Errico, L. Fallani, M. Fattori, C. Fort, M. Zaccanti, G. Modugno, M. Modugno, and M. Inguscio, Anderson localization of a non-interacting bose-einstein condensate, Nature (London) **453**, 895 (2008).
[41] G. Modugno, Anderson localization in boseeinstein condensates, Rep. Prog. Phys. **73**, 102401 (2010).
[42] P. W. Anderson, Absence of diffusion in certain random lattices, Phys. Rev. **109**, 1492 (1958).
[43] S. Aubry and G. André, Analyticity breaking and anderson localization in incommensurate lattices, Ann. Israel Phys. Soc. **3**, 18 (1980).
[44] J. Biddle and S. Das Sarma, Predicted Mobility Edges in One-Dimensional Incommensurate Optical Lattices: An Exactly Solvable Model of Anderson Localization, Phys. Rev. Lett. **104**, 070601 (2010).
[45] X. Cai, L.-J. Lang, S. Chen, and Y. Wang, Topological Superconductor to Anderson Localization Transition in One-Dimensional Incommensurate Lattices, Phys. Rev. Lett. **110**, 176403 (2013).
[46] W. DeGottardi, D. Sen, and S. Vishveshwara, Majorana Fermions in Superconducting 1d Systems Having Periodic, Quasiperiodic, and Disordered Potentials, Phys. Rev. Lett. **110**, 146404 (2013).
[47] S. Ganeshan, J. H. Pixley, and S. Das Sarma, Nearest Neighbor Tight Binding Models with an Exact Mobility Edge in One Dimension, Phys. Rev. Lett. **114**, 146601 (2015).
[48] F. Liu, S. Ghosh, and Y. D. Chong, Localization and adiabatic pumping in a generalized Aubry-André-Harper model, Phys. Rev. B **91**, 014108 (2015).
[49] J. Wang, X.-J. Liu, G. Xianlong, and H. Hu, Phase diagram of a non-abelian Aubry-André-Harper model with p-wave superfluidity, Phys. Rev. B **93**, 104504 (2016).

[50] Y. Cao, X. Gao, X.-J. Liu, and H. Hu, Anderson localization of cooper pairs and majorana fermions in an ultracold atomic fermi gas with synthetic spin-orbit coupling, Phys. Rev. A **93**, 043621 (2016).

[51] J. C. C. Cestari, A. Foerster, and M. A. Gusmão, Fate of topological states in incommensurate generalized Aubry-André models, Phys. Rev. B **93**, 205441 (2016).

[52] Q.-B. Zeng, S. Chen, and R. Lü, Generalized Aubry-André-Harper model with p-wave superconducting pairing, Phys. Rev. B **94**, 125408 (2016).

[53] X.-D. Bai, J. Wang, X.-J. Liu, J. Xiong, F.-G. Deng, and H. Hu, Polaron in a non-abelian Aubry-André-Harper model with p-wave superfluidity, Phys. Rev. A **98**, 023627 (2018).

[54] H. Yao, H. Khoudli, L. Bresque, and L. Sanchez-Palencia, Critical Behavior and Fractality in Shallow One-Dimensional Quasiperiodic Potentials, Phys. Rev. Lett. **123**, 070405 (2019).

[55] H. Yao, T. Giamarchi, and L. Sanchez-Palencia, Lieb-Liniger Bosons in a Shallow Quasiperiodic Potential: Bose Glass Phase and Fractal Mott Lobes, Phys. Rev. Lett. **125**, 060401 (2020).

[56] F. A. An, K. Padavić, E. J. Meier, S. Hegde, S. Ganeshan, J. Pixley, S. Vishveshwara, and B. Gadway, Observation of tunable mobility edges in generalized Aubry-André lattices, arXiv:2007.01393.

[57] Q.-B. Zeng, S. Chen, and R. Lü, Anderson localization in the non-Hermitian Aubry-André-Harper model with physical gain and loss, Phys. Rev. A **95**, 062118 (2017).

[58] T. Liu, H. Guo, Y. Pu, and S. Longhi, Generalized Aubry-André self-duality and mobility edges in non-Hermitian quasiperiodic lattices, Phys. Rev. B **102**, 024205 (2020).

[59] Q.-B. Zeng, Y.-B. Yang, and Y. Xu, Topological phases in non-Hermitian Aubry-André-Harper models, Phys. Rev. B **101**, 020201(R) (2020).

[60] N. Hatano and D. R. Nelson, Localization Transitions in Non-Hermitian Quantum Mechanics, Phys. Rev. Lett. **77**, 570 (1996).

[61] N. Hatano and D. R. Nelson, Vortex pinning and non-Hermitian quantum mechanics, Phys. Rev. B **56**, 8651 (1997).

[62] N. Hatano and D. R. Nelson, Non-Hermitian delocalization and eigenfunctions, Phys. Rev. B **58**, 8384 (1998).

[63] R. Hamazaki, K. Kawabata, and M. Ueda, Non-Hermitian Many-Body Localization, Phys. Rev. Lett. **123**, 090603 (2019).

[64] Z. Gong, Y. Ashida, K. Kawabata, K. Takasan, S. Higashikawa, and M. Ueda, Topological Phases of Non-Hermitian Systems, Phys. Rev. X **8**, 031079 (2018).

[65] C. Mejía-Cortés and M. I. Molina, Interplay of disorder and $\mathcal{PT}$ symmetry in one-dimensional optical lattices, Phys. Rev. A **91**, 033815 (2015).

[66] D. M. Jović, C. Denz, and M. R. Belić, Anderson localization of light in $\mathcal{PT}$-symmetric optical lattices, Opt. Lett. **37**, 4455 (2012).

[67] Y. N. Joglekar, D. Scott, M. Babbey, and A. Saxena, Robust and fragile $\mathcal{PT}$-symmetric phases in a tight-binding chain, Phys. Rev. A **82**, 030103(R) (2010).

[68] C. H. Liang, D. D. Scott, and Y. N. Joglekar, $\mathcal{PT}$ restoration via increased loss and gain in the $\mathcal{PT}$-symmetric Aubry-André model, Phys. Rev. A **89**, 030102(R) (2014).

[69] C. Yuce, $\mathcal{PT}$ symmetric Aubry-Andre model, Phys. Lett. A **378**, 2024 (2015).

[70] Y. N. Joglekar and A. Saxena, Robust $\mathcal{PT}$-symmetric chain and properties of its hermitian counterpart, Phys. Rev. A **83**, 050101(R) (2011).

[71] D. D. Scott and Y. N. Joglekar, Degrees and signatures of broken $\mathcal{PT}$ symmetry in nonuniform lattices, Phys. Rev. A **83**, 050102(R) (2011).

[72] A. K. Harter, T. E. Lee, and Y. N. Joglekar, $\mathcal{PT}$-breaking threshold in spatially asymmetric Aubry-André and Harper models: Hidden symmetry and topological states, Phys. Rev. A **93**, 062101 (2016).

[73] See Supplemental Material at http://link.aps.org/supplemental/10.1103/PhysRevA.103.L011302 for details of the (I) analytical investigation of the system's symmetry, (II) $\langle \mathrm{MIPR} \rangle$ and $\langle r \rangle$ near the center of the spectrum, (III) technical details of our multifractal analysis, and for (IV) a possible experimental realization of our model.

[74] L. Schäfer and F. Wegner, Lattice instantons, a basis for a treatment of localized states? Z. Phys. B **39**, 281 (1980).

[75] G. H. Zhang and D. R. Nelson, Eigenvalue repulsion and eigenvector localization in sparse non-Hermitian random matrices, Phys. Rev. E **100**, 052315 (2019).

[76] V. Oganesyan and D. A. Huse, Localization of interacting fermions at high temperature, Phys. Rev. B **75**, 155111 (2007).

[77] A. Pal and D. A. Huse, Many-body localization phase transition, Phys. Rev. B **82**, 174411 (2010).

[78] H. Hiramoto and M. Kohmoto, Scaling analysis of quasiperiodic systems: Generalized harper model, Phys. Rev. B **40**, 8225 (1989).

[79] Y. Takasu, T. Yagami, Y. Ashida, R. Hamazaki, Y. Kuno, and Y. Takahashi, PT-symmetric non-Hermitian quantum many-body system using ultracold atoms in an optical lattice with controlled dissipation arXiv:2004.05734.